Boiling Heat Transfer of Nitrogen in a Thermosyphon Condenser-Reboiler

Seiichi Sakaue
Nippon Sanso Corp., Tsukuba, Ibaraki 300-26, Japan

An experimental investigation was conducted to determine the boiling heat-transfer characteristics in a thermosyphon condenser-reboiler of air-separation plants. The test section was a plate-fin heat exchanger of practical size of 0.106 m width and 2.56 m length. The testing fluid was nitrogen. Experiments were carried out within a range of pressure from 150 to 300 kPa, submergence from 1.95 to 2.80 m, and heat flux up to 11 kW/m^2 under constant wall-temperature condition. The liquid superheat at the onset of boiling was rather significant. The boiling heat-transfer coefficients obtained agreed well with Chen's correlation modified by Colburn's J factor within a mean deviation of 9.3%.

Introduction

Brazed-aluminum plate-fin heat exchangers have been widely used in industrial cyrogenic processes such as air-separation plants. The heat exchangers in air-separation plants are operated at a low temperature difference and low heat flux. This is especially true in condenser-reboilers, where the fluids change their phases within the very small temperature range of 1 to 2 K. Therefore, high accuracy and reliability of the prediction method of heat-transfer characteristics are required for designing effective and efficient heat exchangers in the condenser-reboiler.

The objective in this series of studies is to characterize the heat-transfer performance of the plate-fin heat exchangers in thermosyphon condenser-reboilers for air-separation plants. In principle, the condenser-reboiler has two loops thermally interconnected by the plate-fin heat exchangers, that is, a boiling loop and a condensing loop. Thus the heat-transfer process becomes essentially an operation under constant wall-temperature condition, one that characterizes the present system. This article is focused on the heat-transfer characteristic in the boiling loop.

For many years, experimental studies have been conducted on the convective boiling in a plate-fin passage, generally under constant heat flux condition (e.g., Robertson, 1979, 1983). However, Robertson's correlation (1983) overpredicts the experimental data obtained by this study, as shown in Figure 1. On the other hand, only a few studies of boiling heat transfer have been carried out with a constant wall-temperature condition. This is mainly because of the difficulty in the estimation of heat flux. Recently, Beduz and Scurlock (1994) showed that a distinct difference existed in the heat-transfer characteristics of plate-fin heat exchangers of laboratory size and those of practical size. This finding suggests the importance of experimental investigations on obtaining, in the design process, a suitable boiling heat-transfer coefficient in plate-fin heat exchangers of practical size with a constant wall-temperature condition.

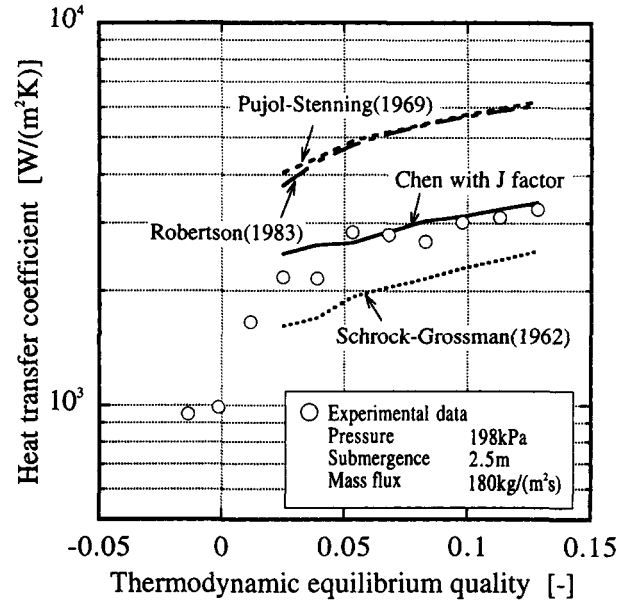

Figure 1. Comparison of existing correlations with experimental data.

Thus, a heat-transfer experiment was conducted using a thermosyphon condenser-reboiler of nitrogen with plate-fin heat exchanger of practical size.

By introducing a thermal-resistance layer, and a highly precise and accurate temperature measurement system, the boiling heat transfer of nitrogen in a plate-fin passage was investigated. This article describes the fundamental feature of the boiling heat transfer in such a condenser-reboiler and presents reliable correlation for practical use.

Experiment

Experimental apparatus

A diagram of the experimental apparatus is shown in Figure 2. This system has two main loops for boiling and condensation. Each loop is connected thermally in the test section of the plate-fin heat exchanger. Vessel 1 of the boiling loop, test section, and vessel 2 of the condensing loop were set vertically in a 2.6-m×2.6-m×8.5-m cold box that was thermally insulated with perlite powders from the ambient.

In the boiling loop, subcooled liquid nitrogen from vessel 1 first passed through a venturi flowmeter and was introduced into the bottom of the test section. This subcooled liquid nitrogen was heated in the test section by the condensing stream, and the resulting two-phase mixture was returned to vessel 1. The vapor from the top of vessel 1 was discharged to the atmosphere, keeping the vessel pressure constant with a control valve. The liquid level in vessel 1, or submergence, was maintained automatically by regulating the liquid supply from the liquid nitrogen storage.

The condensing loop was a closed loop. The nitrogen vapor generated with an electric heater in vessel 2 was introduced to the top of the test section and was condensed through the test section. The condensed nitrogen was then returned to vessel 2.

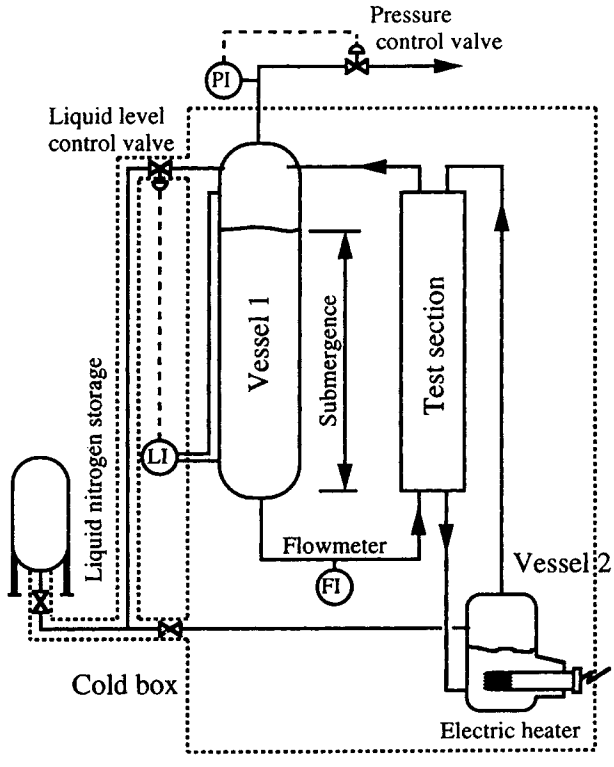

Figure 2. Experimental apparatus.

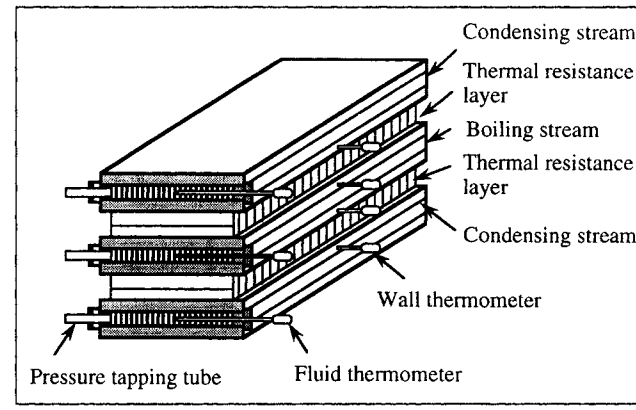

Figure 3. Cross section of test section.

Test section

A cross section of the test section is shown in Figure 3. The test section was 2.56 m long and consisted of three rectangular passages, one boiling and two condensing, with an internal dimension of height, 6.4 mm, and width, 106 mm. The corrugated fins were plain and were formed from a 0.3-mm-thick aluminum sheet with 472 corrugations per meter. A passage contained 11 sections of corrugated fins along the test section, and each section was 230 mm long with a small gap between each adjacent section.

These passages were separated by thermal-resistance layers 27 mm thick, consisting of fins and separating plates. These thermal-resistance layers were equipped to measure the heat flux from the condensing stream to the boiling stream. Fins of the thermal-resistance layer were set perpendicular to the fluids passages. The separating plates, which were usually thin in the practical heat exchanger, were thick enough, in this case, to insert the thermometers.

Instrumentation

The pressure drop along the test section was measured by means of 12 pressure taps per passage. The connection from each pressure tap to the pressure transducer was made with a 3-mm-OD stainless-steel tube that was set horizontally to eliminate the influence of the static head of liquid, and that extended out of the cold box. The differential pressure transducer (Validyne Engineering Corp., Model DP15) with an accuracy of ±0.25% FS was connected to any two taps. In addition, the absolute pressure transducers (Setora Systems Inc., Model 204) with an accuracy of ±0.11% FS were installed at the inlet taps of the test section.

Fluid and wall temperatures in the test section were measured by 80 thermometers of platinum resistance thermometer sensors (JIS1604-1989 Pt100 Tolerance Class A) set within 1.6-mm-diameter stainless-steel tubes. A digital multimeter was used to measure these resistances, and the resolution and the accuracy were 0.1 mΩ and 3 mΩ at 20 Ω, respectively. Because the accurate measurement of very small temperature differences in the test section was essential for determin-

ing the heat-transfer coefficients, considerable attention was paid to the selection and the calibration of the thermometers. All thermometers were calibrated against a standard platinum resistance thermometer with an accuracy of 0.05 K, by the IPTS-68 method. Then the precision and accuracy of the thermometers were within 0.01 K and 0.07 K, respectively.

Fluid temperatures were measured at the inlet and outlet positions by thermometers inserted into the gaps. Wall temperatures were measured by thermometers set in holes drilled in the separating plate at half-thickness, and these pockets were filled with the silicon grease to ensure good thermal contact.

The flow rate of the boiling stream was measured by a venturi flowmeter. On the other hand, the flow rate of the condensing stream was estimated from the power input of the electric heater and the latent heat of nitrogen.

All signals were directed to a personal computer through a GPIB interface, and the data were analyzed immediately.

Experiments

Preliminary experiment

Prior to the thermosyphon experiments, a single vapor-phase heat transfer and pressure drop were measured for the plate-fin passage using nitrogen gas at room-temperature and low-temperature conditions. The average heat-transfer coefficient in the nth section, h_n, was determined by the heat-balance relationship. Providing the heat-transfer coefficient is uniform around the periphery of the subchannel, the heat-transfer coefficient is determined by

$$m \cdot \Delta i_n = h_n \cdot (A_{pn} + \eta_{Fn} \cdot A_{sn})(T_{wn} - T_{fn}), \tag{1}$$

where Δi_n is the enthalpy change in the nth section calculated from the measured temperature and pressure, and η_F is the fin efficiency given by (Kays and London, 1984, p. 16)

$$\eta_F = \frac{\tanh(s)}{s}, \tag{2}$$

where

$$s = \frac{H_F}{2}\left[\frac{2h}{\lambda_F \cdot t_F}\right]^{0.5}. \tag{3}$$

In Figure 4, the measured heat-transfer characteristics were plotted in terms of Colburn's J factor, J_H, against Reynolds number (Re). Colburn's J factor is defined as follows:

$$J_H = \frac{h \cdot Pr^{2/3}}{\dot{m} \cdot c_p}. \tag{4}$$

The friction factor given by the following equation is also shown in Figure 4:

$$f = \frac{1}{2}\Delta p \cdot \frac{\rho_G}{\dot{m}^2} \cdot \frac{D_h}{L}, \tag{5}$$

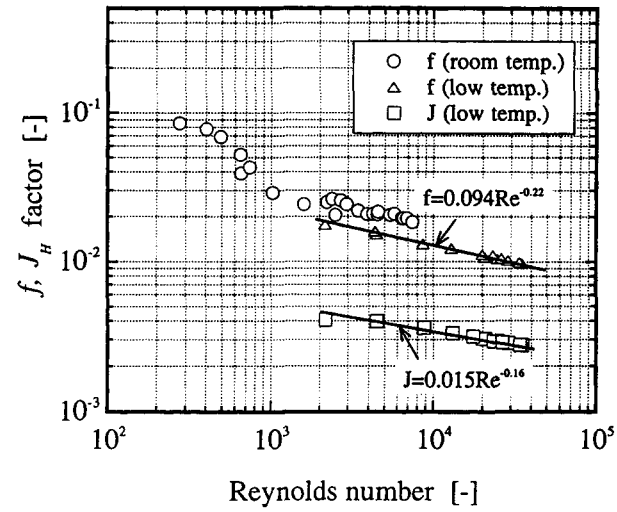

Figure 4. Relationship between Reynolds number and f, and J factor for the testing passage.

where D_h is the hydraulic equivalent diameter based on the wetted perimeter. The curves indicated in Figure 4 are of the form

$$J_H = a_1 \cdot Re^{b_1} \tag{6}$$

and

$$f = a_2 \cdot Re^{b_2}. \tag{7}$$

The constants a and b were determined by the least-square curve fitting on the single-phase data, and for plain-fin passage in the turbulent region, the values of $a_1 = 0.015$, $b_1 = -0.16$ and $a_2 = 0.094$, $b_2 = -0.22$ were obtained.

The thermal-resistance layer is quite important for determining the boiling heat-transfer coefficients and the thermodynamic equilibrium quality of the thermosyphon stream. The heat balance between the boiling passage and the condensing passage is defined by the following equation.

$$Q_n/A_1 = -c_n \cdot \lambda_n \cdot \Delta T_{rn} \tag{8}$$

where Q_n is the heat input, ΔT_{rn} is the temperature difference across the thermal-resistance layer, A_1 is the surface area of the separating plate, and c_n is the calibration constant. This constant is, in general, a geometric factor, and is able to calculate on the basis of geometrical dimensions of the thermal-resistance layer. Because this constant significantly affects the accuracy of the heat-transfer coefficient, calibration of the thermal-resistance layer was carried out to determine the constant in Eq. 8. This could also be established by using a flow of nitrogen gas under low-temperature conditions. The calibration constant, c_n, was determined at every 11 sections along the test section, which confirmed that the thermal resistance between the boiling passage and the condensing passage were uniform within a deviation of $\pm 2.5\%$ along the test section.

Thermosyphon experiment

Heat-transfer measurement was conducted in the boiling loop as well as in the condensing loop. This article, however, mainly describes the boiling heat transfer. The experimental ranges in the present boiling experiment were the pressure from 150 to 300 kPa, the submergence from 1.95 to 2.80 m, and the heat flux up to 11 kW/m^2. The experimental setup was, at first, brought to a predetermined steady state, and then various parameters, such as pressure, temperature, and mass flow rate, were measured.

The average value of the boiling heat-transfer coefficient was determined at every 11 sections along the test section of the heat balance by Eq. 9:

$$-c_n \cdot \lambda_n \cdot \Delta T_{rn} \cdot A_1 = h_n \cdot (A_{pn} + \eta_{Fn} \cdot A_{sn})(T_{wn} - T_{fn}). \quad (9)$$

Temperature differences between the wall and the stream were measured, and the heat flux was determined based on the temperature difference across the thermal resistance layer by using Eq. 8 and the calibration constants, c_n.

The local thermodynamic equilibrium quality, x_n, is calculated by the following equation:

$$x_n = \frac{i_{fn} - i^*_{Ln}}{i^*_{GLn}}, \quad (10)$$

where i_{fn} is the specific enthalpy of the thermosyphon stream at the measuring point, and i^*_{GLn} is the latent heat of vaporization.

Results and Discussion

Temperature profile

An example of a measured temperature profile along the test section is shown in Figure 5 against the distance from the bottom of the test section. The circles and triangles represent the measured fluid temperatures and the measured wall temperatures, respectively. The dash-dotted lines represent the saturation temperatures calculated by the measured pressures at 12 points along the passage. The saturation temperatures were found to be in good agreement with the measured fluid temperatures to within 0.05 K in the saturated region. The thermodynamic equilibrium quality, x, is also shown in Figure 5. The quality is taken to be zero at the point of intersection, B, of the profile of the fluid temperature in the subcooled liquid region and that of the saturation temperature.

For the boiling passage, subcooled liquid nitrogen was introduced into the bottom of the test section, point A. The temperature of the boiling fluid increased along the test section and reached saturation at point B. However, it continued to rise due to a certain amount of superheat. After point C, the fluid temperature dropped to the saturation temperature, and the fluid temperature decreased gradually toward the top of the test section according to the static pressure change. Cryogenic fluids with such high superheat in the boiling initiation region is not peculiar, and has been reported elsewhere (Robertson, 1979). The single-phase region occupied approximately 20–30% of the test section in the present experiment. This suggests the importance of the prediction of the onset of saturated boiling.

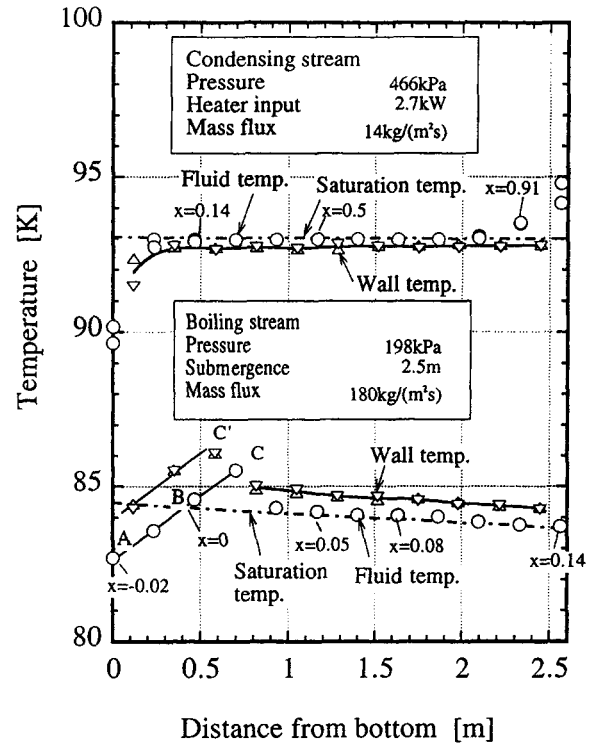

Figure 5. Temperature profile in the test section.

On the other hand, the fluid temperature indicates the superheated vapor condition at the top of the test section. During condensation, the fluid temperature coincides, of course, with the saturation temperature, and then the condensate at the outlet becomes the subcooled liquid. The temperature difference between the boiling and the condensing loop is about 8 K in this case. This large temperature difference is caused by the thermal-resistance layer. It should be noted that the actual heat exchanger has no thermal-resistance layer, and therefore the temperature difference reduces to about 1 to 2 K.

Boiling heat-transfer coefficient

Measured values of the boiling heat-transfer coefficients were plotted against the thermodynamic equilibrium quality in Figure 6. In the low-quality region, the heat-transfer coefficient was a weak function of the quality and/or the mass flux. However in the high-quality region, the heat-transfer coefficient increased significantly with the increase in the quality and the mass flux.

The dependence of the heat-transfer coefficient on pressure was not seen in the present range of 150–300 kPa.

Comparison with existing correlations

The boiling heat-transfer coefficients obtained by the experimental data shown in Figure 5 were plotted against the quality in Figure 1. As the temperature difference between fluid and wall is very small, the experimental error significantly affects the error of the heat-transfer coefficient. For example, an experimental error of 0.05 K results in an error of approximately 10% of the heat-transfer coefficient. And

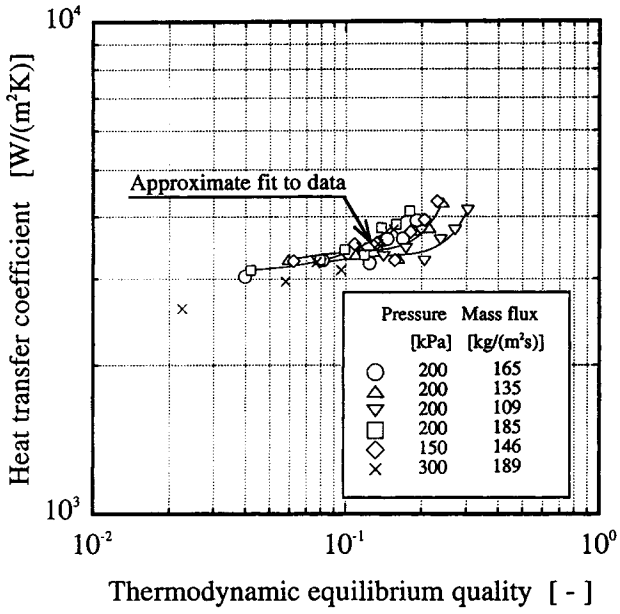

Figure 6. Relationship between boiling heat-transfer coefficient and quality.

the heat-transfer coefficient is compared with the coefficients predicted using the following correlations:

1. Chen's correlation with Colburn's J factor
2. Schrock–Grossman's correlation (1962)
3. Pujol–Stenning's correlation (1969)

Chen's correlation is modified by using Colburn's J factor in the calculation of the convective term as follows. Chen proposed that the boiling heat-transfer coefficient, h_b, was assumed to be given by the sum of the convective term, h_{con}, and the nucleate boiling term, h_{nuc} (Chen, 1966).

$$h_b = h_{nuc} + h_{con}. \tag{11}$$

In the original correlation, the convective term was calculated from the Dittus–Boelter-type equation, which was applied, in general, to round tubes. In this study with the specific geometry such as plate-fin passage (Mandrusiak and Carey, 1989), the convective term was calculated by the following equation:

$$h_{con} = J_{HL} \cdot \dot{m} \cdot c_{pL} \cdot Pr^{-2/3} \cdot F \cdot (1-x), \tag{12}$$

where J_{HL} represents Colburn's J factor, and the boiling enhancement factor, F, is traditionally postulated to be a function of the reciprocal of the Lockhart–Martinelli parameter, $1/X$. The reciprocal of the Lockhart–Martinelli parameter is the square root of the ratio of the vapor-phase pressure gradient to the liquid-phase pressure gradient, and is given in this study by the following equation:

$$\frac{1}{X} = \frac{x}{1-x} \cdot \left(\frac{f_G \cdot \rho_L}{f_L \cdot \rho_G} \right)^{0.5}, \tag{13}$$

where the friction factors of each phase are given by Eq. 5. The value of F is estimated from the graph proposed by Chen (1966).

The nucleate boiling term is predicted by using the pool boiling correlation of Forster and Zuber (1955), as suggested by Chen (1966).

$$h_{nuc} = 0.0122 \frac{\lambda_L^{0.79} \cdot c_{pL}^{0.45} \cdot \rho_L^{0.49}}{\sigma^{0.5} \cdot \mu_L^{0.29} \cdot i_{GL}^{0.24} \cdot \rho_G^{0.24}} \cdot \Delta T^{0.24} \cdot \Delta p^{0.75} \cdot S, \tag{14}$$

where Δp is the difference in saturation pressure corresponding to the wall superheat. The suppression factor, S, introduced by Chen, takes into account the nucleate boiling suppression by forced convection, which is given as a function of the effective Reynolds number for two-phase fluid, as has been given by Chen.

The previously mentioned correlation is referred to in this article as the modified Chen's correlation. The experimental data are compared with this modified Chen's correlation and the other representative correlations in Figure 1. As Figure 1 shows, the modified Chen's correlation is in good agreement with the experimental data, except the very low-quality region, while Schrock–Grossman's correlation underpredicts these data, and Pujol–Stenning's correlation overpredicts them. All of the experimental data are compared with the modified Chen's correlation in Figure 7.

The mean absolute deviation was given by

$$D = \frac{1}{N} \sum_{i=1}^{N} \left| \frac{h_{calc} - h_{meas}}{h_{calc}} \right| \times 100, \tag{15}$$

where N was the number of experimental data. The mean absolute deviation of this correlation is estimated from the experimental data to be 9.3%. Results of the comparison with existing correlations are summarized in Table 1. It is evident that the modified Chen's correlation provides the best agreement with the experimental data.

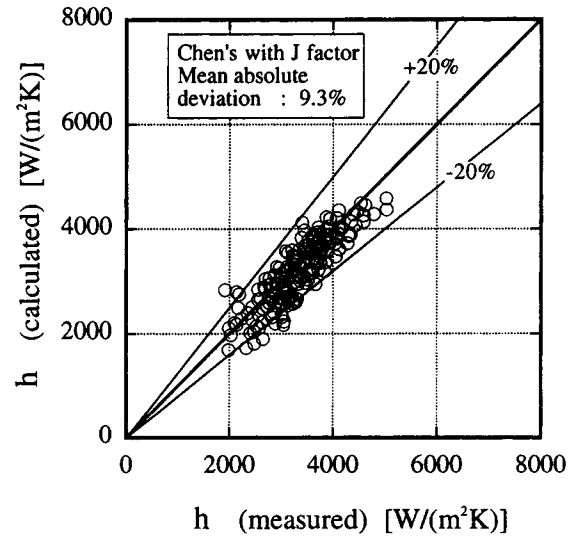

Figure 7. Comparison of the experimental data with modified Chen's correlation with Colburn's *J* factor.

Table 1. Deviations of the Boiling Heat Transfer Correlations from Experimental Data

Correlation	Mean Abs. Dev. [%]
Modified Chen's	9.3
Schrock–Grossman's	32.6
Pujol–Stenning's	43.4

Conclusion

An experimental investigation was conducted to determine the boiling heat-transfer characteristics of nitrogen in a plate-fin thermosyphon condenser-reboiler using the high precision and accuracy of the temperature measurement system. The results obtained in this study can be summarized as follows:

1. The liquid superheat was significant at the onset of boiling, which should be taken into account in the design of the heat exchanger.

2. In the saturated boiling region, the boiling heat-transfer coefficients can be successfully predicted by the modified Chen's correlation with Colburn's J factor.

The condensing heat-transfer characteristics of nitrogen will be presented in the near future.

Acknowledgment

The author would like to thank Mr. H. Kawakami and Dr. M. Ozawa for their valuable discussions in this research program, and Nippon Sanso Corp. for permission to publish this paper.

Notation

A_p = primary surface area, m^2
A_s = secondary surface area, m^2
c_p = specific heat at constant pressure, J/(kg·K)
f = friction factor
H_F = fin height, m
L = passage length, m
m = mass flow rate, kg/s
$\dot{m}$ = mass flux, kg/(m^2·s)
Pr = Prandtl number
T = temperature, K
λ = thermal conductivity, W/(m·K)
ρ = density, kg/m^3
σ = surface tension, N/m
μ = viscosity, Pa·s

Subscripts

cal = calculated value
f = fluid
G = vapor
L = liquid
mea = measured value
sat = saturation condition
w = wall

Literature Cited

Beduz, C., and R. G. Scurlock, "The Mismatch between Laboratory Boiling Heat Transfer Data and Industrial Requirements," *Cryogenics*, **34**, 373 (1994).

Chen, C. C., "Correlations for Boiling Heat Transfer to Saturated Fluids in Convective Flow," *Ind. Eng. Chem. Process Des. Dev.*, **5**, 322 (1966).

Forster, H. K., and N. Zuber, "Dynamics of Vapor Bubbles and Boiling Heat Transfer," *AIChE J.*, **1**, 531 (1955).

Kays, W. M., and A. L. London, *Compact Heat Exchangers*, 3rd ed., McGraw-Hill, New York (1984).

Mandrusiak, G. D., and V. P. Carey, "Convective Boiling in Vertical Channels with Different Offset Strip Fin Geometries," *Trans. ASME, J. Heat Transfer*, **111**, 156 (1989).

Pujol, L., and A. H. Stenning, "Effect of Flow Direction on the Boiling Heat Transfer Coefficient in Vertical Tubes," *Symp. Ser. of Can. Soc. for Chem. Eng.*, No. 1, Plenum Press, New York, p. 401 (1969).

Robertson, J. M., "Boiling Heat Transfer with Liquid Nitrogen in Brazed-Aluminum Plate-Fin Heat Exchangers," *AIChE Symp. Ser.*, **75**(189), 151 (1979).

Robertson, J. M., "The Boiling Characteristics of Perforated Plate-fin Channels with Liquid Nitrogen in Upflow," *ASME HTD*, **27**, 35 (1983).

Schrock, V. E., and L. M. Grossman, "Forced Convection Boiling in Tubes," *Nucl. Sci. Eng.*, **12**, 474 (1962).

Manuscript received Mar. 28, 1996, and revision received Aug. 19, 1996.